



EXPPERIMENTAL STUDY AND MODELING OF COUPLED HEAT AND MOISTURE TRANSFERS IN CEMENT MORTAR

A. Chikhi ^{a,b*}, A. Belhamri ^b, P. Glouannec ^c and A. Magueresse ^c

^aDépartement de Génie Civil, Faculté de Technologie, Université Sétif 1, 19000 Algérie

^bLaboratoire de Génie Climatique, Faculté des Sciences de la Technologie, Université Constantine 1, 25000 Algérie

^cLaboratoire d'Ingénierie des MATériaux de Bretagne, Université de Bretagne Sud, Rue de Saint Maudé, 56321 Lorient Cedex France

*E-mail address: a.chikhi@yahoo.fr

Abstract

In spite of the broad use of cement mortar in construction field, its hygrothermal behavior is not clarified, up to now, satisfactorily, especially under the particular conditions of its use. A study is carried out on a block of cement mortar subjected to variations in temperature and humidity. Numerical and experimental approaches are used. For both approaches, the ambient conditions have a direct impact on the behavior of the wall. In parallel to the experimental approach, a model representative of heat and mass transfer, in multiphasic medium (cement mortar), is developed in order to predict hygrothermal behavior of the wall. This model is validated by confrontation of simulated and experimental results. This study would enable us to make an adequate design of the construction walls according to the climatic parameters.

Keywords: Cement mortar, porous medium, behavior, experimentation, modeling.

1. Introduction

Most materials used in the construction of buildings are porous. A portion or possibly the totality of these pores is interconnected, making them permeable with the vapor water. This moisture, in addition to the problems of durability which it is likely to cause [1-4], can also influence the thermal performances appreciably. Therefore, the adequate modeling of the phenomenon of transport in the porous environments presents an essential interest to numerically simulate the behavior of the walls of construction subjected to periodic changes of the climatic parameters.

We work, in this study, on an instrumented block of cement mortar subjected to changes in temperature and humidity. The recorded measurements are compared with the numerical results in order to validate them. A study also of the relative humidity sensitivity inside the sample with respect to the mass transfer coefficient is made.

In the end, taking into account the adverse effects that condensation in the mass may cause, a checking of this phenomenon is made by numerical simulation.

2. Presentation of the Physical Model

The first tests of modeling - as that of Glaser [5] - have only taken into account the transfer in phase vapor in order to study the risks of condensation in the walls; they suppose negligible the transfer in liquid phase. However, the incomplete character of these approaches led the researchers to elaborate some works describing in a more precise way this phenomenon of coupled transfers [6-13]. These include the model developed by Philip and De Vries-[14-17], which is chosen to conceive the present work because it allows a good description and a better understanding of physical phenomena, gives

good results and faithfully restores most of the phenomena observed in laboratory for homogeneous mediums, isotropic, slightly hygroscopic [11].

In the case of a monodimensional representation of the exchanges, and in the case of following assumptions of modeling:

- the solid phase constituting the porous media is homogeneous, undeformable and isotropic,
- the various phases are in thermal and hygroscopic balance,
- the gas phase obeys the law of perfect gases,
- there is no chemical reaction,
- the density of the liquid phase is constant,
- the effects of gravity are neglected,

If we think in terms of saturation instead of water content as mentioned in the literature cited above, the system of equations of Philip-De-Vries model is written:

$$\begin{cases} \varepsilon \frac{\partial S}{\partial t} = \frac{\partial}{\partial x} \left[\varepsilon (D_{Sl} + D_{Sv}) \frac{\partial S}{\partial x} + (D_{Tl} + D_{Tv}) \frac{\partial T}{\partial x} \right] & (1) \\ \rho c \frac{\partial T}{\partial t} = \frac{\partial}{\partial x} \left(\lambda \frac{\partial T}{\partial x} \right) + \rho_l L_v \frac{\partial}{\partial x} \left(D_{Tv} \frac{\partial T}{\partial x} + \varepsilon D_{Sv} \frac{\partial S}{\partial x} \right) & (2) \end{cases}$$

The degree of water saturation (S) is defined like the ratio of the volume of water contained in the pores on the volume of the open pores. It is related to the mass moisture content by the following relation [18]:

$$S = \frac{w \rho_s}{\varepsilon \rho_l} \quad (3)$$

• **Mass Transfer Coefficient D_S :**

D_S is the sum of the liquid water transfer coefficient and that of the vapor water under the effect of a saturation gradient:

$$D_S = D_{Sl} + D_{Sv} \quad (4)$$

D_{Sl} and D_{Sv} are calculated from the following expressions [19]:

✓ *Liquid water transfer coefficient:*

$$D_{Sl} = \frac{k_{rl}}{\varepsilon \cdot \mu_l} \left(-\frac{\partial P_c}{\partial S} \right) \quad (5)$$

Several authors proposed empirical relations to determine the permeability relating to water and gases. Laghcha [20] shows in his work that for cementing materials, the permeability relating to the liquid can be determined in the following way:

$$k_{rl} = \sqrt{S} \left[1 - \left(1 - S^{1/m} \right)^m \right]^2 ; m = 1/2.1 \quad (6)$$

In the same way, the capillary pressure (P_c) can be calculated according to saturation [21]:

$$P_c = a(S^{-2.27} - 1)^{(1-m)} ; a = 20.45. 10^6 \quad (7)$$

✓ *Vapor water transfer coefficient:*

$$D_{Sv} = \frac{D_{eff} M P_{vsat}}{\rho_l R T \varepsilon} \left(\frac{\partial f}{\partial S} \right) \quad (8)$$

Where D_{eff} is the effective coefficient of diffusion and f is a function which depends on capillary pressure and temperature, they are calculated as follows [19]:

$$D_{eff} = D_{vap} (1 - S^2) [\varepsilon (1 - S)]^{4/3} \quad (9)$$

$$f = \exp \left(- \frac{P_c M}{\rho_l R T} \right) \quad (10)$$

Lastly, the saturating vapor pressure P_{vsat} is determined by the following relation:

$$P_{vsat} = 611 \exp \left(\frac{17.27 T}{T + 237.3} \right); P_{vsat} \text{ in [Pa] and } T \text{ in } [^\circ\text{C}] \quad (11)$$

3. Experimental study

3.1. Studied material

Cement mortar is a building compound created by mixing sand and a selection of aggregates with a specified amount of water. It can be used for a number of applications.

Mortar has been used for centuries as a means of adhering bricks or concrete blocks to one another. It continues to be used in many different types of construction. Professional building projects often employ mortar as the binder between bricks in walls, fences, and walkways. Around the house, it is often employed to make quick repairs in patio slabs and reset loosened stones or bricks in a walkway or retaining wall.

Cement mortar also makes an excellent medium for creating a smooth surface to walls made from bricks and other forms of masonry. It is applied with the use of a trowel and then smoothed into position. Often, the application is conducted in more than one coat, making it possible to slowly achieve a covering that adheres properly to the wall surface. The mortar may be tinted in order to add a small amount of color to the façade or paint can be added as a topcoat at a later date.

The ingredients in cement mortar vary somewhat, depending on the manufacturer specifications. For this study, the detained composition is described in “table1”.

Table1. Initial composition of studied material

<i>Mass fraction</i>	<i>Cement</i>	<i>Sand</i>	<i>Water</i>	<i>Water/Cement</i>
	0.222	0.666	0.111	0.5

After mixing the various components (sand, cement and water), the mortar is versed in a wooden parallelepipedic mould of 25cm on sides and 5cm on depth.

With the same mixture, other samples of smaller size (13x13x2 cm³) were made. These plates were used for the measurement of some material thermo physical properties. It is of thermal conductivity, the specific heat and the density “table 2”. The porosity is drawn from the bibliography [22].

Table2. Properties of studied material for a temperature ranging between 0 and 50°C

<i>Density</i> (<i>kg.m⁻³</i>)	<i>Porosity</i> (-)	<i>Thermal conductivity</i> (<i>W.m⁻¹.K⁻¹</i>)	<i>Specific heat</i> (<i>J.kg⁻¹.K⁻¹</i>)
2200	0.18	1.6	850

3.2. Description of the device of measurement

The sample of cement mortar, kept in its lacquered wooden mould, is isolated on all sides except on a vertical face in order to approaching adiabatic conditions and thus obtaining a monodimensional heat flow. Moisture and temperature sensors, distributed on the various elements of the experimental benches, are connected to a station of acquisition, itself connected to a computer. Two experiments are made:

3.2.1 First experiment

This block is placed, in upright position, in an oven during a few days to be heated at a temperature of 40 °C, and then cooled at ambient temperature by opening of the oven door.

The measurement of the temperatures of various surfaces of the sample "T2 to T6" is ensured by thermocouples stuck to the wooden mould, T1 and Th2 by jacketed thermocouples inserted into the material during the casting, that of the not insulated face "Tp", by a pyrometer. The temperatures of the air inside the oven are measured by jacketed thermocouples distributed in this medium "Ta1 to Ta4". A sensor of the type "rotronic" (Sa) is used to measure the temperature and the relative humidity of the air in the oven. Lastly, in order to distribute the air in the oven well and to thus standardize the temperature, a small ventilator is placed inside this one (“Fig. 1 and 2”, “Table 3”).

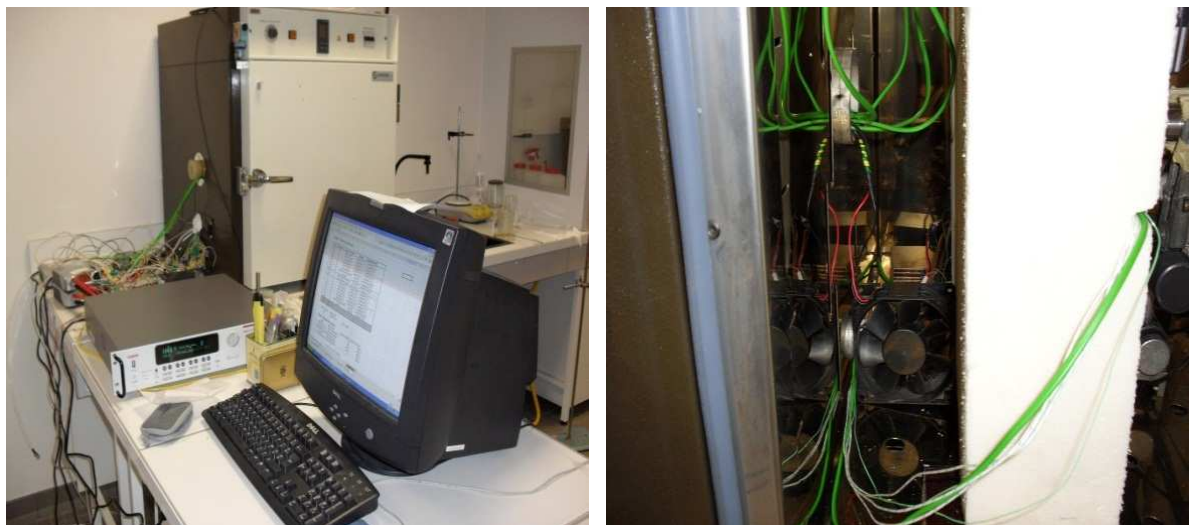


Figure1: The experimental device
(Experiment 1)

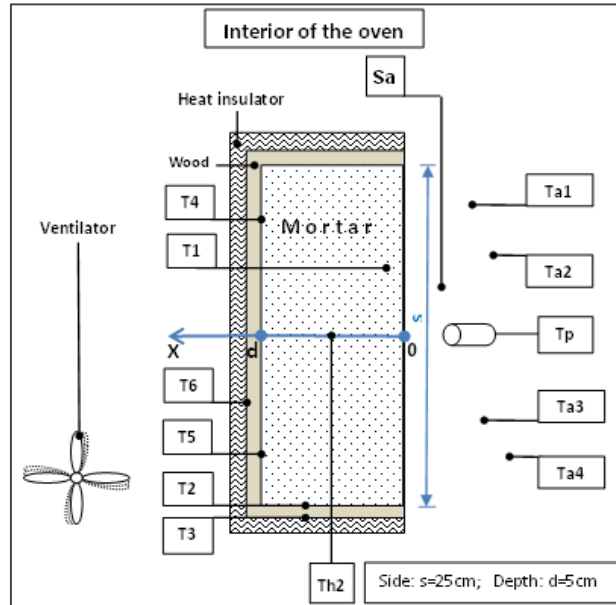


Figure2: Block diagram of the measurement device and sensors implantation (Experiment 1)

3.2.2 Second experiment

The block is fitted in an upright position also, inside a box. Humidification is obtained by spray water injection in the air ranging between the bottom of the box and the face not isolated of the sample.

The measurement of the temperatures of isolated sides of the sample "T2 to T6" is ensured by thermocouples stuck to the wooden mould, that of the face in direct contact with the air "T7", by another stuck to the mortar, temperature "T1" by a jacketed thermocouple in stainless (inox) inserted into the material during the casting. In parallel, to know the temperature and humidity inside the sample, three sensors "S1 to S3" are inserted in the sample at 1 cm of the bottom, at the medium and at 1 cm of surface, respectively. Some measurements of humidity and temperature of the air are realized by a sensor placed in space separating the bottom of the box and the face not isolated from the mortar "S4" ("Fig. 3 and 4", "Table3").



Figure3: The experimental device (Experiment 2)

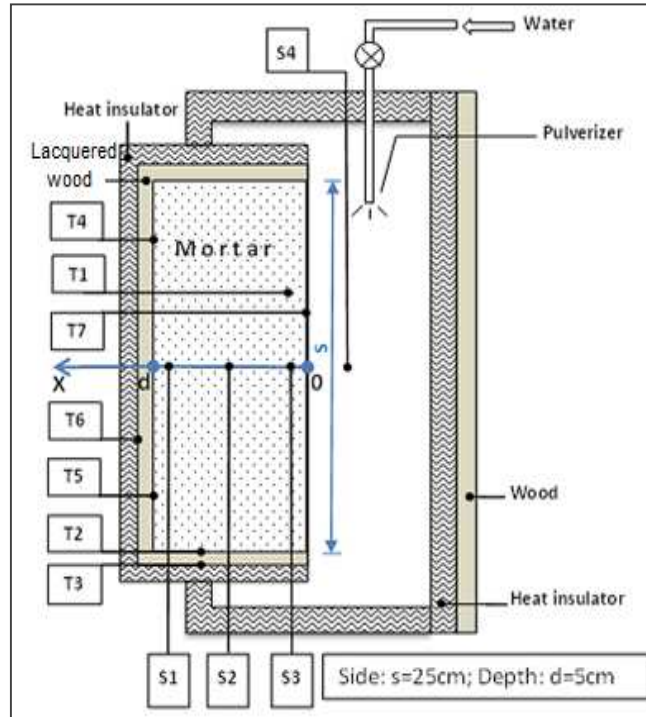


Figure4: Block diagram of the measurement device and sensors implantation (Experiment 2)

3.2.3 Nomenclature of the sensors

“Table3” gives the designation of the sensors, their position and the parameters which they measure.

Table3. Designation and position of the connected sensors

<i>Des</i>	<i>Connected sensor</i>	<i>Measure</i>	<i>Position</i>	<i>Observation</i>
<i>T1</i>	<i>Thermocouple (K)</i>	<i>Temperature [°C]</i>	<i>Drowned into the mortar at $x= 1\text{ cm}$</i>	<i>Experiments: 1 and 2</i>
<i>T2</i>	<i>Thermocouple (K)</i>	<i>Temperature [°C]</i>	<i>Side position: interface mortar-wood</i>	<i>Experiments: 1 and 2</i>
<i>T3</i>	<i>Thermocouple (K)</i>	<i>Temperature [°C]</i>	<i>Side position: interface wood-insulator</i>	<i>Experiments: 1 and 2</i>
<i>T4</i>	<i>Thermocouple (K)</i>	<i>Temperature [°C]</i>	<i>At the bottom: interface mortar-wood ($x=5\text{cm}$)</i>	<i>Experiments: 1 and 2</i>
<i>T5</i>	<i>Thermocouple (K)</i>	<i>Temperature [°C]</i>	<i>At the bottom: interface mortar-wood ($x=5\text{cm}$)</i>	<i>Experiments: 1 and 2</i>
<i>T6</i>	<i>Thermocouple (K)</i>	<i>Temperature [°C]</i>	<i>At the bottom: interface wood-insulator</i>	<i>Experiments: 1 and 2</i>
<i>Th2</i>	<i>Thermocouple (K)</i>	<i>Temperature [°C]</i>	<i>Drowned into the mortar at $x=2.5\text{cm}$</i>	<i>Experiment 1</i>
<i>Ta1</i>	<i>Thermocouple (K)</i>	<i>Temperature [°C]</i>	<i>In ambient air of the oven</i>	<i>Experiment 1</i>
<i>Ta2</i>	<i>Thermocouple (K)</i>	<i>Temperature [°C]</i>	<i>In ambient air of the oven</i>	<i>Experiment 1</i>
<i>Ta3</i>	<i>Thermocouple (K)</i>	<i>Temperature [°C]</i>	<i>In ambient air of the oven</i>	<i>Experiment 1</i>
<i>Ta4</i>	<i>Thermocouple (K)</i>	<i>Temperature [°C]</i>	<i>In ambient air of the oven</i>	<i>Experiment 1</i>
<i>Tp</i>	<i>Pyrometer</i>	<i>Temperature [°C]</i>	<i>Temperature measurement of surface</i>	<i>Experiment 1</i>
<i>Sa</i>	<i>Sensor (type : Rotronic)</i>	<i>Temperature [°C] + Humidity [%]</i>	<i>In ambient air of the oven</i>	<i>Experiment 1</i>
<i>T7</i>	<i>Thermocouple (K)</i>	<i>Temperature [°C]</i>	<i>At the surface of the sample ($x=0$)</i>	<i>Experiment 2</i>
<i>S1</i>	<i>Sensor (type : Sensirion)</i>	<i>Temperature [°C] + Humidity [%]</i>	<i>Drowned into the mortar at $x= 4\text{cm}$</i>	<i>Experiment 2</i>
<i>S2</i>	<i>Sensor (type : Sensirion)</i>	<i>Temperature [°C] + Humidity [%]</i>	<i>Drowned into the mortar at $x=2.5\text{cm}$</i>	<i>Experiment 2</i>
<i>S3</i>	<i>Sensor (type : Sensirion)</i>	<i>Temperature [°C] + Humidity [%]</i>	<i>Drowned into the mortar at $x= 1\text{ cm}$</i>	<i>Experiment 2</i>
<i>S4</i>	<i>Sensor (type : Sensirion)</i>	<i>Temperature [°C] + Humidity [%]</i>	<i>In the air: between the exchanger and the sample</i>	<i>Experiment 2</i>

3.2.4 Data acquisition

The K thermocouples are connected to a data acquisition (standard: Keithley 2700) which performs the analog-to-digital conversion of the signals. A National Instrument is used for the “sensirion” sensors. These two devices are connected to a microcomputer “Fig. 5”. Acquisition is managed by the software "LabVIEW" with a time of 2 seconds examination and a step of 10 minutes recording.



Figure 5: Chain of acquisition

4. Results and discussion

4.1. Sequence of measurement

“Fig. 6 and 7” present the evolution of temperature and relative humidity for the two experiments mentioned above. By applying a rise of temperature in the oven, one observes a rise of the air’s temperature, followed by a temperature in the various points of measurement “Fig. 6”. The weak variation in temperature between the surface of the sample and the bottom is due to the great value of thermal conductivity ($1.6 \text{ W m}^{-1} \text{ K}^{-1}$) and to a thickness of the relatively small block (5cm). “Fig. 7” shows the capacity of the cement mortar to absorb and desorb the moisture of the air with which it is in contact, the response of Hr within material is quick. Measures of internal humidity “Fig. 7” indicate that the material reacts to the fluctuations of the air’s humidity with a more significant delay for the deepest points than for those close to surface.

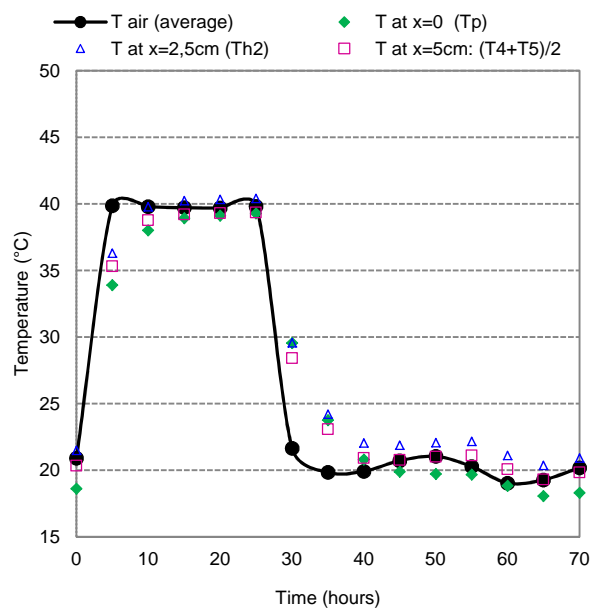


Figure 6: Variation of temperature and relative humidity during the first experiment

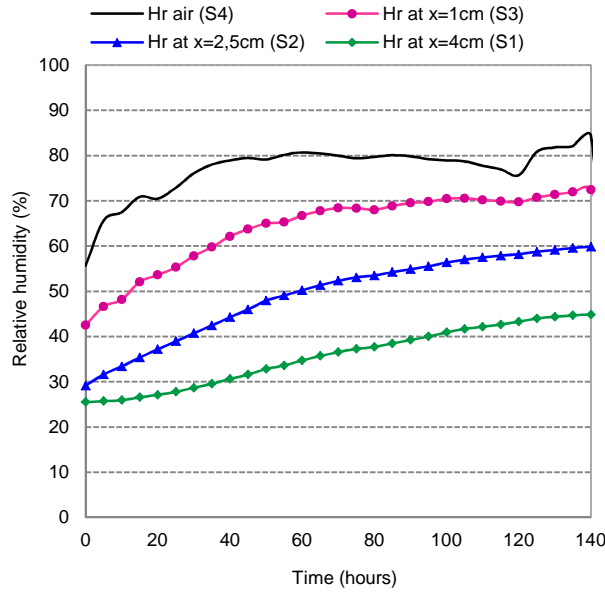


Figure 7: Variation of relative humidity during the second experiment

4.2. Confrontation simulation/experience

➤ Boundary conditions

In order to carry a comparison (numeric simulation /experiment), both temperature and relative humidity of the air are extracted each step of time from the experiment's real conditions.

- **Mass transfer**

At $x=0$:

$$-\left(\varepsilon D_S \frac{\partial S}{\partial x} + D_T \frac{\partial T}{\partial x}\right)_{x=0} = \frac{h_m}{\rho_l} (\rho_{v,\infty} - \rho_{v,x=0}) \quad (12)$$

At the other limits (at $x = d$), surface is supposed to be impermeable (waterproof lacquered wood – “Fig. 4”), the mass flow, which crosses it, is thus null.

- **Heat transfer**

At $x = 0$:

$$-\left(\lambda \frac{\partial T}{\partial x}\right)_{x=0} - (L_v j_v)_{x=0} = (h_c + h_r)(T_\infty - T_{x=0}) + L_v h_m (\rho_{v,\infty} - \rho_{v,x=0}) \quad (13)$$

On the bottom, on the insulated face, i.e. when $x=d$, the temperature is imposed. It is the average temperature measured by the thermocouples "T4" and "T5" “Fig. 4”.

➤ Initial conditions

For the same reason cited above, the initial conditions applied to the model are also extracted from the real conditions of the experiment.

4.2.1 Evolution of temperature and relative humidity

For the calculation of relative humidity inside material - or the activity as many researchers call it-, we referred to the catalogue of the materials' properties created by the institute Bauphysik of Fraunhofer [23]. The activity is transformed at correlation according to saturation by method GAB.

In order to reproduce the experimental results and to validate the model suggested to simulate the behavior of this material, a simulation reproducing the experimental conditions is carried out.

“Fig. 8 and 9” show the evolution according to the time of the temperature and the relative humidity of the air as well as various depths of the block. A comparison is carried out; there is a good agreement between the computed values and those measured. In “Fig. 8”, the coincidence of certain curves is due to the difficulty in imposing in experiments a significant variation in temperature between the surface and the bottom of the sample. Nevertheless, the model reproduces development and displacement of moisture and temperature front.

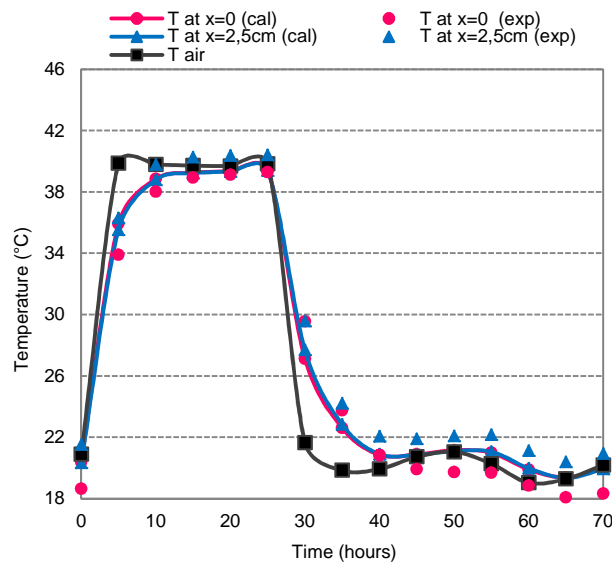


Figure 8: Evolution of temperature: comparison between model and experiment (Experiment 1)

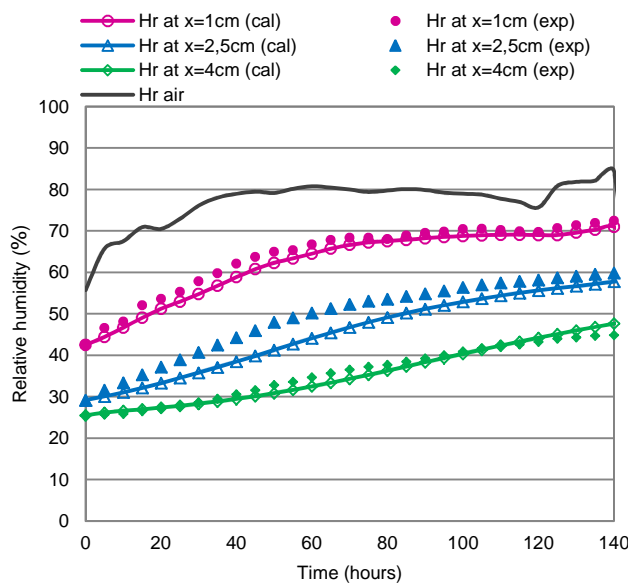


Figure 9: Evolution of relative humidity: comparison between model and experiment (Experiment 2)

4.2.2 Profile of temperature and relative humidity

Confrontation between the results of simulation and those of the experiment of temperature and relative humidity profiles inside material is represented on “Fig. 10 and 11” for three times chosen arbitrarily. The maximum change between calculation and experiment is approximately 1.5 °C for the temperature “Fig. 10” and 6 % for the relative humidity “Fig. 11”, which allows concluding on good capabilities of the model to predict the material behavior under variable hygrothermal conditions.

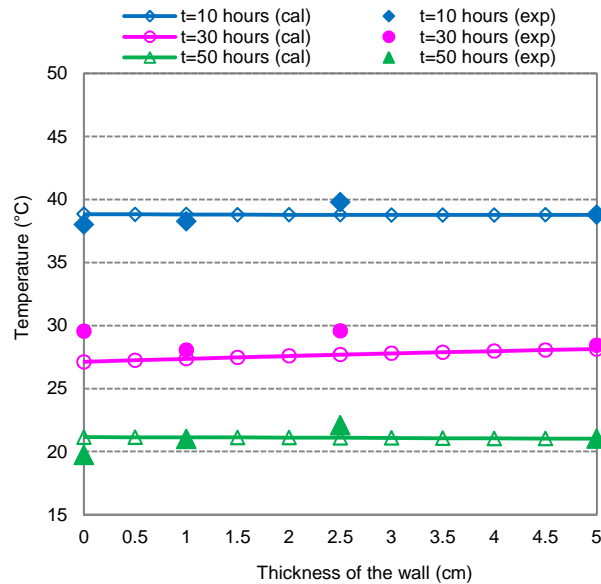


Figure 10: Profile of temperature: comparison between model and experiment (Experiment 1)

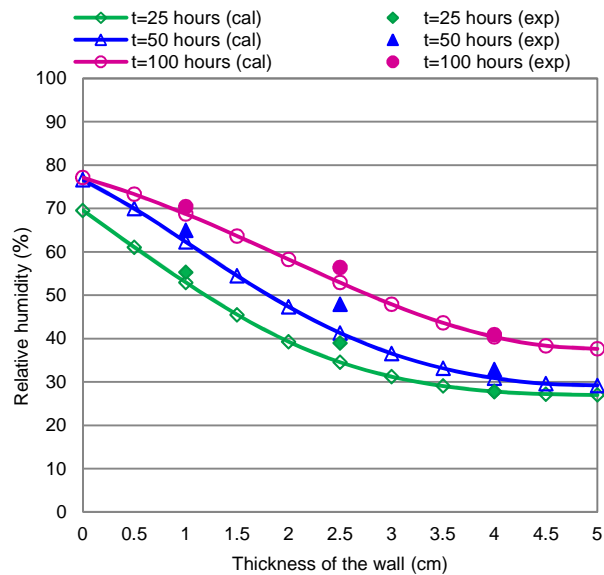


Figure 11: Profile of relative humidity: comparison between model and experiment (Experiment 2)

4.3. Sensitivity of the relative humidity

In order to study the model sensitivity with respect to the mass transfer coefficient (D_S), three cases were treated, the first by considering this coefficient variable (according to saturation and temperature) and calculate it from "Eq. (4) to Eq. (11)"; while for the two other cases, it is supposed to be constant by affecting two different values to him draw from the bibliography [24]. The three

curves obtained by simulation are compared with that obtained in experiment “Fig. 12”. The relative humidity for a variable mass transfer coefficient agrees better with the experimental result, from where necessity to calculate D_s at each steps of time and not to consider it constant. That also made it possible to validate the expressions used for calculation of the mass transfer coefficient.

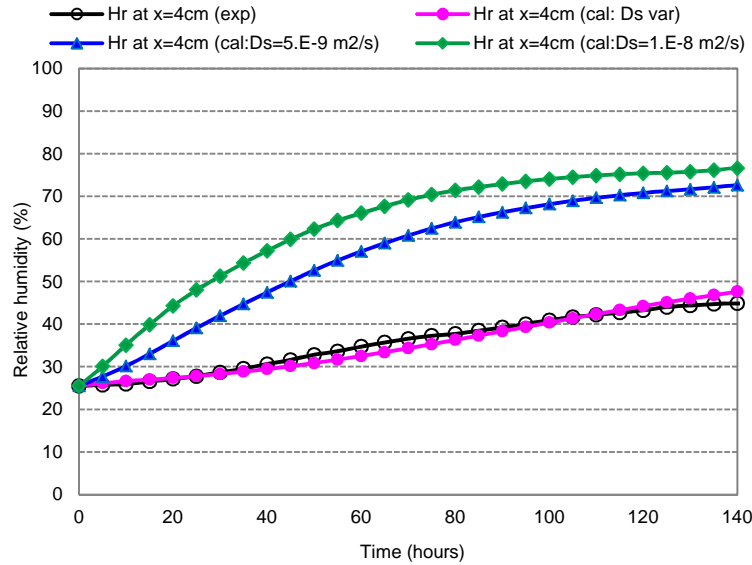


Figure12: Relative humidity evolution for different values of mass transfer coefficient (Experiment 2)

4.4. Checking of condensation in the mass

Certain building materials are hygroscopic i.e. they are ready to fix moisture, capillary condensation is formed quickly even for moistures relative weak, which can induce modifications of their physical characteristics, in particular mechanical and thermal. It is then necessary to check this phenomenon of condensation in order to limit the degradation of materials being able to involve on the one hand a structural weakening and on the other hand a variation of their thermo-physical properties.

By determining the vapor pressures (P_v and $P_{v,sat}$) in each node of volume of control, condensation inside the wall can be checked.

P_v is calculated starting from the following expression:

$$P_v = H_r P_{v,sat} \quad (14)$$

The capillary depression ($-P_c$) is connected to the relative humidity via the well-known equation of Kelvin:

$$-P_c = \frac{RT\rho_l \cdot \ln(H_r)}{M} \quad (15)$$

So:

$$H_r = \exp\left(\frac{-P_c M}{RT\rho_l}\right) \quad (16)$$

“Fig. 13” represents the evolution in time of P_v and P_{vsat} of three points to various depths of material, the saturated vapor pressures are confused in this test because of their very close corresponding temperatures; and all three superiors to the partial pressures, which results in concluding that there is not risk of condensation in the mass for this case.

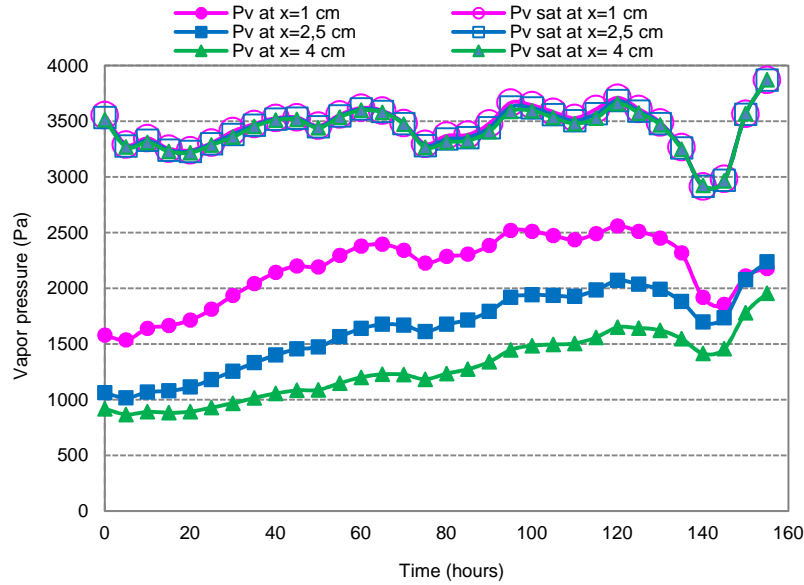


Figure13: Checking of condensation in the mass (Experiment 2)

5. Conclusions

In this paper, tests are carried out on a material very much used in construction, it is a cement mortar, made in the form of a block and subjected to variations in temperature and relative humidity of the ambient air. Starting from the initial conditions and the real limits of experiment, a numerical simulation is performed also. The confrontation of the results shows a good agreement between experiment and calculation for the various treated cases.

The mass transfer coefficient used is not obtained from direct measurements, but it is built, taking into account specific properties of the material, which are measured independently. It depends on a lot of saturation and temperature.

This study will allow making a design of walls according to the particular climatic conditions which they will be subjected. The model used in this paper can be applied to other types of building materials under real conditions of use. It is therefore possible to improve the thermal performance and thus to save the energy used. Moreover, it will be able to avoid the risks of condensation in the mass and the adverse effects which result from this.

Notations

- c Specific heat, $J.kg^{-1}.K^{-1}$
- D_T Mass transfer coefficient due to the temperature gradient, $m^2.s^{-1}.K^{-1}$
- D_S Mass transfer coefficient due to the saturation gradient, $m^2.s^{-1}$
- D_{Tl} Liquid phase transfer coefficient due to the temperature gradient, $m^2.s^{-1}.K^{-1}$
- D_{Tv} Vapor phase transfer coefficient due to the temperature gradient, $m^2.s^{-1}.K^{-1}$
- D_{Sl} Liquid phase transfer coefficient due to the saturation gradient, $m^2.s^{-1}$
- D_{Sv} Vapor phase transfer coefficient due to the saturation gradient, $m^2.s^{-1}$

D_{vap}	Diffusivity coefficient of the vapor in the air, $m^2 \cdot s^{-1}$
D_{eff}	Effective diffusivity coefficient of vapor, $m^2 \cdot s^{-1}$
H_r	Relative humidity, %
h_c	Convective heat transfer coefficient, $W \cdot m^{-2} \cdot K^{-1}$
h_r	Radiative heat transfer coefficient, $W \cdot m^{-2} \cdot K^{-1}$
h_m	Mass transfer coefficient, $m \cdot s^{-1}$
k	Intrinsic permeability, m^2
k_{rl}	Relative permeability
L_v	Latent heat of vaporization, $J \cdot kg^{-1}$
M	Mass molar, $kg \cdot mol^{-1}$
P_c	Capillary pressure, Pa
R	Gas constant, $J \cdot mol^{-1} \cdot K^{-1}$
S	Saturation
T	Temperature, K or $^{\circ}C$
t	Time, s
P_{vsat}	Saturated vapor pressure, Pa

Greek symbols

ε	Porosity
ρ	Density, $kg \cdot m^{-3}$
λ	Thermal conductivity, $W \cdot m^{-1} \cdot K^{-1}$
μ	Dynamic viscosity of water, $kg \cdot m^{-1} \cdot s^{-1}$
θ	Volume moisture content

Subscripts / Superscripts

a	Air
l	Liquid
v	Vapor
s	Solid

References

- [1] Piaia, J.C.Z., Cheriaf, M., Rocha, J.C. and Mustelier, N.L., Measurements of water penetration and leakage in masonry wall: Experimental results and numerical simulation. *Build. Environ.*, 61, 18-26, 2013.
- [2] Wyrwal, J. and Marynowicz, A., Vapour condensation and moisture accumulation in porous building wall. *Build. Environ.*, 37(3), 313-318, 2002.
- [3] Mlakar, J. and Strankar, J., Temperature and humidity profiles in passive-house building blocks. *Build. Environ.*, 60, 185-193, 2013.
- [4] Dal Pont, S., Lien entre la perméabilité et l'endommagement dans les bétons à haute température, *PhD thesis*, Ecole Natl. Ponts Chaussées, France, 2004.
- [5] Glaser, H., Grafisches vehren zur untersuchung von diffusion-vorgängen, *Kaptechnik*, 11, 345-355, 1959.
- [6] Abahri, K., Belarbi, R. and Trabelsi, A., Contribution to analytical and numerical study of combined heat and moisture transfers in porous building materials. *Build. Environ.* 46 (7), 1354 - 1360, 2011.
- [7] Talukdar, P., Olutmayin, S.O., Osanyintola, O.F. and Simonson C.J., An experimental data set for benchmarking 1-D, transient heat and moisture transfer models of hygroscopic building materials. Part I: Experimental facility and material property data. *Int. J. Heat Mass Transf.*, 50, 4527-4539, 2007.

- [8] Hagentoft, C.E., Kalagasidis, A.S., Adl-Zarrabi, B., Roels, S., Carmeliet, J., Hens, H. 'and al', Assessment method of numerical prediction models for combined heat, air and moisture transfer in building components, benchmarks for one-dimensional cases, *J. Therm. Environ. Build. Sci.*, 27 (4), 327–352, 2004.
- [9] Kunzel, H.M. and Kiessl, K., Calculation of heat and moisture transfer in exposed building components, *Int. J. Heat Mass Transf.*, 40 (1), 159–167, 1997.
- [10] Haupl, P., Grunewald, J., Fechner, H. and Stopp, H., Coupled heat air and moisture transfer in building structures, *Int. J. Heat Mass Transf.*, 40 (7), 1633–1642, 1997.
- [11] Bories, S., Transferts de chaleur et de masse dans les matériaux, analyse critique des différents modèles mathématiques utilisés, *L'humidité dans le bâtiment, Séminaire de l'UNESCO*, France, 1982, 23-25 Novembre, p.13-32.
- [12] Whitaker, S., Simultaneous heat, mass and momentum transfer in porous media – A theory of drying in porous media, *Adv. Heat Transf.*, 13, 119-200, 1977.
- [13] Chen, Z.Q. and Shi, M.H., Study of heat and moisture migration properties in porous building materials, *Appl. Therm. Engineering*, 25, 61-71, 2005.
- [14] Philip, J.R. and De-Vries, D.A., Moisture movement in porous materials under temperature gradients, *Transactions of the American Geophysical Union*, 38(2), 222-232, 1957.
- [15] Crausse, P., Laurent, J.P. and Perrin, B., Influence des phénomènes d'hystérésis sur les propriétés hydriques de matériaux poreux, *Rev. Gen. Therm.*, 35, 95-106, 1996.
- [16] Mendes, N., Philippi, P.C. and Lamberts, R., A new mathematical method to solve highly coupled equations of heat and mass transfer in porous media, *Int. J. Heat Mass Transf.*, 45, 509-518, 2002.
- [17] Crausse, P., Etude fondamentale des transferts couplés de chaleur et d'humidité en milieu poreux non saturé, *PhD thesis*, Institut Natl. Polytech., Toulouse, France, 1983.
- [18] Salagnac, P., Glouannec, P. and Lecharpentier, D., Numerical modeling of heat and mass transfer in porous medium during combined hot air, infrared and microwaves drying, *Int. J. Heat Mass Transf.*, 47, 4479–4489, 2004.
- [19] Belhamri, A., Etude des transferts de chaleur et de masse à l'interface d'un milieu poreux au cours du séchage, *PhD thesis*, University Poitiers, France, 1992.
- [20] Laghcha, A., Contribution à l'étude des transferts gazeux et liquide au sein des parois en béton endommagées sous sollicitation thermo-hydrique. *PhD thesis*, Ecole Dr. Sci. Ing., Lyon, France, 2006.
- [21] Billard, Y., Contribution à l'étude des transferts de fluides au sein d'une paroi en béton. *PhD thesis*, Ecole Dr. Sci. Ing., Lyon, France, 2003.
- [22] Da Chen, Modélisation du comportement hydromécanique d'un mortier sous compression et dessiccation, *PhD thesis*, University Lille, France, 2005.
- [23] Catalogue of material properties, Rep. Annex XIV, Volume 3: Condensation and Energy, International Energy Agency, Energy Conservation in Building and Community Systems, 1991.
- [24] Picandet, V., Influence d'un endommagement mécanique sur la perméabilité et sur la diffusivité hydrique des bétons, *PhD thesis*, Ecole Dr. Méc., Therm. et G. Civil, Nantes, France, 2001.